ResearchGate

See discussions, stats, and author profiles for this publication at: https://www.researchgate.net/publication/242333650

Synthesis of Wurtzite Cu 2 ZnGeSe 4 Nanocrystals and their Thermoelectric Properties

ARTICLE *in* CHEMISTRY - AN ASIAN JOURNAL · OCTOBER 2013

Impact Factor: 4.59 · DOI: 10.1002/asia.201300425 · Source: PubMed

CITATIONS
6

READS
38

7 AUTHORS, INCLUDING:

Fei Jiao
Chinese Academy of Sciences
9 PUBLICATIONS **89** CITATIONS
SEE PROFILE

Wei Xu
Chinese Academy of Sciences
508 PUBLICATIONS **7,027** CITATIONS
SEE PROFILE

Yu-Guo Guo
Chinese Academy of Sciences
168 PUBLICATIONS **10,281** CITATIONS
SEE PROFILE

Available from: Fei Jiao
Retrieved on: 17 January 2016

CHEMISTRY
AN ASIAN JOURNAL
ACES
FULL PAPER

DOI: 10.1002/asia.201300425

Synthesis of Wurtzite $Cu_2ZnGeSe_4$ Nanocrystals and their Thermoelectric Properties

Ding-Jiang Xue, Fei Jiao, Hui-Juan Yan, Wei Xu, Daoben Zhu, Yu-Guo Guo,* and Li-Jun Wan*[a]

Dedicated to Professor Chunli Bai on the occasion of his 60th birthday

Abstract: An unusual wurtzite phase of $Cu_2ZnGeSe_4$ (CZGSe) has been discovered and its corresponding nanocrystals (NCs) were synthesized by using a facile hot-injection solution-phase synthesis method. Moreover, the formation mechanism of this new phase of CZGSe, instead of the typically observed stannite structure, has been investigated in detail, which indicates that wurtzite CZGSe, which represents the kinetic phase, could be prepared by using a kinetic growth process without phase transformation into the thermodynamically stable stannite structure during the colloidal synthesis. In addition, the potential of wurtzite CZGSe as a thermoelectric material is demonstrated by characterizing the thermoelectric properties of as-synthesized wurtzite CZGSe NCs. This work allows for a rational manipulation of the NCs with a desired crystal structure through adjusting the thermodynamics and kinetics without using any additives and, because of its simplicity and versatility, it may be extended to the phase-controlled synthesis of other chalcogenide NCs.

Keywords: chalcogens · germanium · nanocrystals · semiconductors · wurtzite

Introduction

Copper-based quaternary chalcogenide nanocrystals (NCs) have attracted tremendous recent attention as the most-promising low-cost alternatives to conventional solar cell materials, such as $Cu(In,Ga)(S,Se)_2$ (CIGS).[1,2] In particular, Cu_2ZnSnS_4 (CZTS) and $Cu_2ZnSnSe_4$ (CZTSe) NCs have received special attention because of their earth-abundant constituents, extremely low toxicity, optimal band gap, and high absorption coefficient.[3–5] In addition, CZTS and CZTSe NCs have been reported to show promising thermoelectric properties, because of their complex structures and different cationic valences, which provide low thermal conductivities and a means of controlling their Fermi level by adjusting their cation ratios, respectively.[6,7] Attracted by their economic advantage and excellent properties, considerable efforts have recently been directed towards the synthesis of CZTS and CZTSe NCs.[3–10] The extensively reported crystal structures of CZTS and CZTSe NCs reveal stannite or kesterite structures, which feature a tetragonal crystal cell.[4,11] In these structures, all of the metal ions have fixed positions in the unit cells. Besides the formation of stable phases, reports on the synthesis of unusual metastable CZTS and CZTSe NCs with a wurtzite structure, which has a hexagonal crystal cell, have recently begun to appear.[12,13] The random distribution of cations throughout the wurtzite structure offers flexibility for stoichiometry control and, consequently, the ability to tune the energy band gap over a wider range for device optimization, as shown in Figure 1.[13] These above investigations of CZTS and CZTSe NCs with different crystal structures have shown that reaction control, including of reaction temperature, reaction time, solvent, capping ligands, and chalcogenide source, is

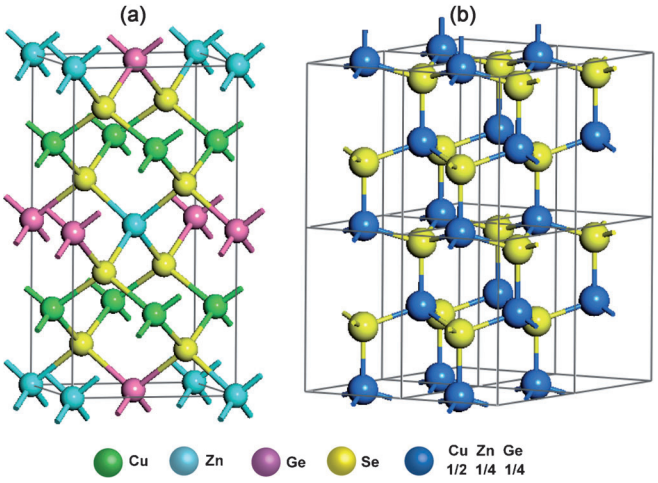

Figure 1. Crystal structures of a) stannite and b) wurtzite CZGSe.

[a] D.-J. Xue, F. Jiao, Dr. H.-J. Yan, Prof. W. Xu, Prof. D. Zhu, Prof. Y.-G. Guo, Prof. L.-J. Wan
Beijing National Laboratory for Molecular Sciences
Institute of Chemistry, Chinese Academy of Sciences (CAS)
Beijing 100190 (P. R. China)
E-mail: ygguo@iccas.ac.cn
wanlijun@iccas.ac.cn

Supporting information for this article is available on the WWW under http://dx.doi.org/10.1002/asia.201300425.

© 2013 Wiley-VCH Verlag GmbH & Co. KGaA, Weinheim

critical for crystal-phase determination. Because the crystal structure of NCs is known to significantly influence their optical and electrical properties,[14–17] it is highly important to explore new controlled pathways for the synthesis of copper-based quaternary chalcogenide NCs with new crystal structures and, in particular, metastable structures, such as wurtzite.

Another potentially attractive—yet not well-studied—quaternary chalcogenide material is $Cu_2ZnGeSe_4$ (CZGSe). CZGSe is a p-type semiconductor with a direct band gap in the range 1.21–1.63 eV, which consists of earth-abundant and low-toxicity elements.[18–20] The properties that arise from its structural complexity and variety of ionic valences make it a potential thermoelectric material. It has recently been reported that CZGSe shows promising thermoelectric properties. The best figure of merit (ZT) value that was obtained from this material so far was 0.55 at 723 K.[18]

In general, one of the most-promising strategies for enhancing the ZT values of thermoelectric materials is to decrease their thermal conductivity by promoting phonon scattering, which can be achieved by decreasing the size of the crystal domains into the nanoscale.[21–24] In this scenario, a hot-injection solution-phase synthesis method, which features the separation of the nucleation and growth stages of the NCs, is particularly well-suited to the production of thermoelectric materials with a high level of control over the size, phase, and composition of the crystallographic nanodomains.[25–28] Recently, Cabot et al. reported the synthesis of CZGSe NCs with a stannite structure by using a hot-injection method.[18] Although the synthesis of wurtzite CZTS and CZTSe NCs has been an increasingly active area of research in recent years, to the best of our knowledge, there have been no reports on the synthesis of CZGSe NCs with a wurtzite structure. Herein, taking the above syntheses of wurtzite CZTS and CZTSe NCs into consideration, we present the first report on the solution-phase synthesis of CZGSe NCs with a wurtzite structure, as well as their thermoelectric properties.

Results and Discussion

Wurtzite CZGSe NCs were synthesized through a hot-injection solution-phase synthesis method. In a typical synthesis of CZGSe NCs with a wurtzite structure, diphenyl diselenide, which has shown recent utility as a facile and low-temperature selenide source for the synthesis of semiconductor NCs, was selected as the selenide source.[13,29] $Cu(Ac)_2$ (0.2 mmol), $Zn(Ac)_2$ (0.2 mmol), and GeI_4 (0.1 mmol) were mixed with oleylamine (OLA, 9 mL) in a three-necked flask and degassed at about 120 °C for 30 min by bubbling with Ar gas under stirring. In a separate two-necked flask, diphenyl diselenide (0.2 mmol) and OLA (1 mL) were degassed at about 120 °C for 30 min by bubbling with Ar gas under stirring, then allowed to cool to 70 °C. The temperature of the former solution was heated to 230 °C, the solution of diphenyl diselenide and oleylamine was quickly injected, and the mixture was maintained at this temperature for 60 min to allow the growth of NCs. Finally, the flask was cooled to RT and excess EtOH was added to precipitate the NCs, which could be harvested through centrifugation at 9000 rpm for 3 min. The precipitates were washed three times with a mixture of EtOH and toluene. The final products were dispersed in toluene for further characterization.

The structure of the as-obtained product was characterized by powder X-ray diffraction (XRD), as shown in Figure 2a (230 °C). We found that the XRD pattern did not match the diffraction pattern of previously reported CZGSe NCs or those in the JCPDS database (JCPDS No. 52-0867). Instead, the experimental XRD pattern could be indexed to a new wurtzite-phase CZGSe. Whilst the crystal cell of stannite CZGSe is an analogue of vertically expanded binary zinc-blende ZnSe, wurtzite CZGSe could be considered as a derivative of wurtzite ZnSe.[12] Therefore, the wurtzite CZGSe crystal cell was constructed starting from the wurtzite ZnSe cell with substitution of the Zn^{2+} lattice positions by a 2:1:1 occupancy probability of Cu^+, Zn^{2+}, and Ge^{4+} cations (see the Supporting Information). In this structure, the selenium anions are hexagonally close-packed, whilst the Cu^{I}, Zn^{II}, and Ge^{IV} cations randomly occupy a half of the interstices of the selenium anions, as shown in Figure 1. The experimental pattern of the CZGSe NCs matches well with

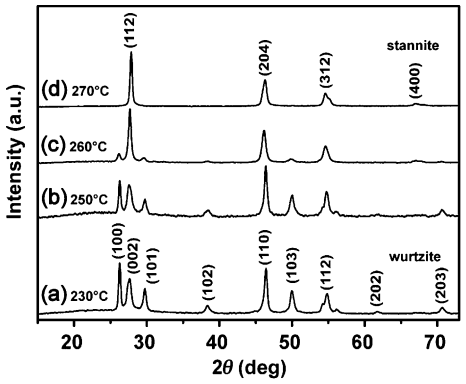

Figure 2. XRD patterns of CZGSe NCs that were synthesized at different reaction temperatures for 60 min: a) 230 °C, b) 250 °C, c) 260 °C, and d) 270 °C.

Abstract in Chinese:

本文通过一种简易的液相热注法合成了纤锌矿结构的 $Cu_2ZnGeSe_4$ (CZGSe) 纳米晶。考察了反应时间、反应温度对纤锌矿结构 CZGSe 纳米晶形成的影响。实验表明纤锌矿结构 CZGSe 是热力学上的亚稳相，为动力学控制产物。探索了纤锌矿结构 CZGSe 纳米晶在热电领域的应用。

© 2013 Wiley-VCH Verlag GmbH & Co. KGaA, Weinheim

the simulated one of a wurtzite structure with $a = 3.90$ Å and $c = 6.49$ Å, thus indicating that such CZGSe NCs adopt a wurtzite crystal structure (see the Supporting Information, Table S1).

To understand the formation mechanism of the wurtzite CZGSe NCs, instead of the most-reported stannite structure, a temperature-dependent phase-evolution process was carefully examined. As shown in Figure 2, the evolution of the structure of the reaction products was characterized by XRD analysis of the synthesized NCs at temperatures from 230 °C to 270 °C for a constant time (60 min). We found that, when the reaction temperature was below 260 °C, the more-disordered wurtzite structure was obtained, rather than the ordered stannite one. On increasing the temperature to 260 °C, the samples contained two crystalline phases, wurtzite and stannite, and the stannite phase was found to be dominant. On further increasing temperature to 270 °C, only the stannite phase was found. These results demonstrated that the phase transformation tended to gradually change from a dominant wurtzite phase into a mixture of stannite and wurtzite and, finally, pure stannite with increasing temperature. On the basis of this above analysis, we propose that wurtzite CZGSe is less thermodynamically stable than the commonly observed tetragonal stannite.

To further confirm this conclusion, structural information about the reaction products after different times during the synthesis was obtained from the XRD data. As shown in Figure 3, four samples were obtained after various reaction

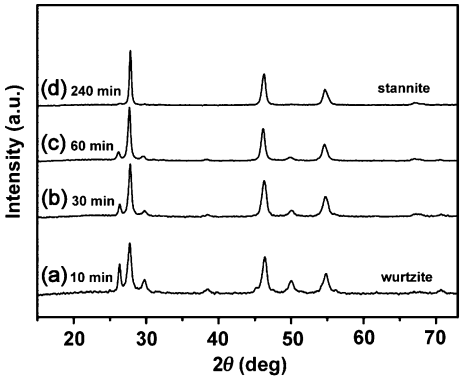

Figure 3. XRD patterns of CZGSe NCs that were synthesized at 260 °C for different reaction times: a) 10 min, b) 30 min, c) 60 min, and d) 240 min.

times at the same temperature (260 °C), ranging from 10 to 240 min. At $t = 10$ min after the injection of the precursor, a pure wurtzite phase was observed. On increasing the time to 30 and 60 min, a mixture of wurtzite and stannite phases appeared. On further prolonging the reaction time to 240 min, only the pure stannite phase was formed. Based on the above variation in peak shape with respect to reaction time, as well as reaction temperature, we can firmly conclude that wurtzite CZGSe is controlled by a kinetic growth process, whereas stannite CZGSe is under thermodynamic control, which could be explained by Ostwald's rule of stages that crystal formation must occur through a series of intermediate crystallographic phases prior to the formation of the final thermodynamically stable structure.[30–33] Therefore, specific reaction control, such as reaction temperature and time, is crucial for synthesizing CZGSe with a thermodynamically metastable wurtzite structure.

Figure 4a shows a typical TEM image of the as-synthesized CZGSe NCs. The CZGSe NCs are slightly polydispersed, with most of the NCs falling within the range 25–

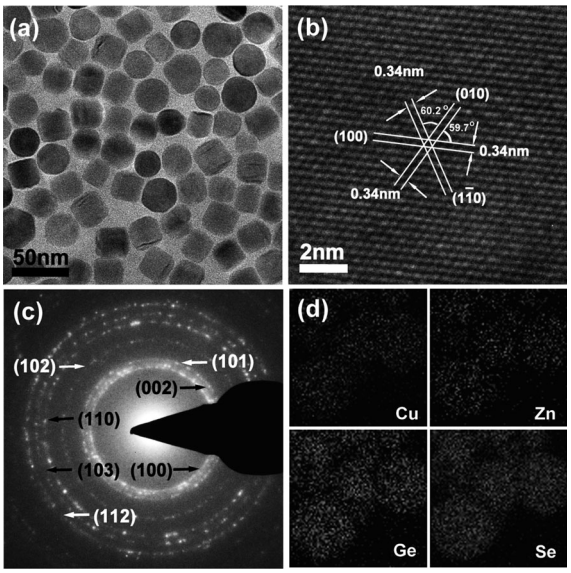

Figure 4. a) TEM image of as-synthesized CZGSe NCs. b) HRTEM image of a single CZGSe NC. c) SAED pattern of as-synthesized CZGSe NCs. d) STEM-EDS elemental maps of Cu, Zn, Ge, and Se, respectively.

30 nm. A high-resolution TEM image (Figure 4b) of an individual CZGSe NC indicates that it is well-crystallized and the lattice spacings of 0.34 nm correspond to the {100} set of planes of wurtzite CZGSe. The selected-area electron diffraction (SAED) pattern (Figure 4c) also reveals that the NCs have a wurtzite structure. The spatial distribution of different compositional elements was obtained by scanning transmission electron microscopy-energy dispersive X-ray spectroscopy (STEM-EDS) elemental mapping. The elemental maps of Cu, Zn, Ge, and Se (Figure 4d) show that all of the compositional elements exist in all of the NCs and exhibit no apparent elemental separation or aggregation, thus indicating that the distributions of all four elements are highly homogeneous within the NCs. Moreover, the composition of the CZGSe NCs was determined by EDS, which corresponded well with the stoichiometry of $Cu_2ZnGeSe_4$ (see the Supporting Information, Figure S1). In addition, X-ray photoelectron spectroscopy (XPS) was performed to investigate the oxidation states of the four constituent elements in the as-synthesized CZGSe NCs (Figure 5). The copper XPS spectrum shows two symmetric peaks at 932.1 and 951.9 eV, with a peak splitting of 19.8 eV, which is char-

© 2013 Wiley-VCH Verlag GmbH & Co. KGaA, Weinheim

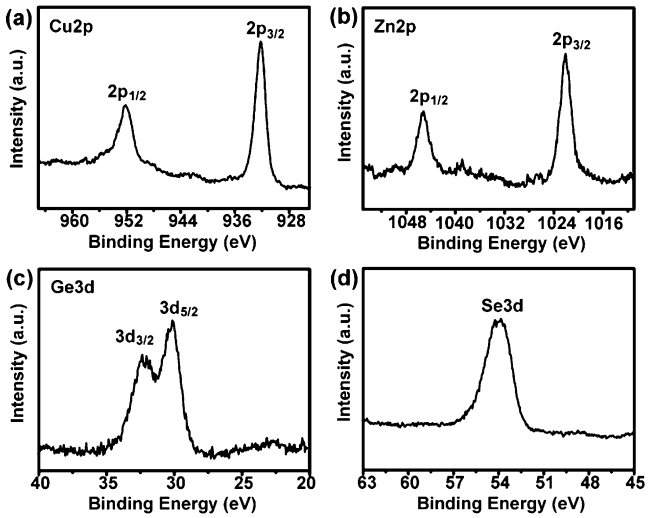

Figure 5. XPS spectra of a) Cu 2p, b) Zn 2p, c) Ge 3d, and d) Se 3d.

acteristic of monovalent copper. The Zn 2p peaks at 1022.1 and 1045.1 eV show a peak separation of 23 eV, consistent with the standard splitting of 22.97 eV, thus suggesting the presence of Zn^{II}. The Ge 3d peaks at 30.1 and 32.4 eV indicate the presence of Ge^{IV}. The Se 3d peak at 53.9 eV indicates the presence of Se^{2-}. These results show that all four elements are in the expected oxidation states for CZGSe.

The thermoelectric properties of wurtzite CZGSe NCs that were synthesized at 230 °C for 60 min were determined and are shown in Figure 6; these measurements were performed within a narrow temperature range to preserve the wurtzite phase. Figure 6a shows the temperature dependence of the Seebeck coefficient of the NCs. The positive Seebeck coefficient indicates that the wurtzite CZGSe NCs are a p-type semiconductor. The Seebeck coefficient measurements show an increasing trend from 48 $\mu V K^{-1}$ at 260 K to 81 $\mu V K^{-1}$ at 400 K. The electrical conductivity (Figure 6b) of the wurtzite CZGSe NCs increases from 5930 $S m^{-1}$ at 260 K to 10953 $S m^{-1}$ at 400 K. These relatively high values confirm the large extent of removal of the surface ligands that are used in the solution processing of the material.

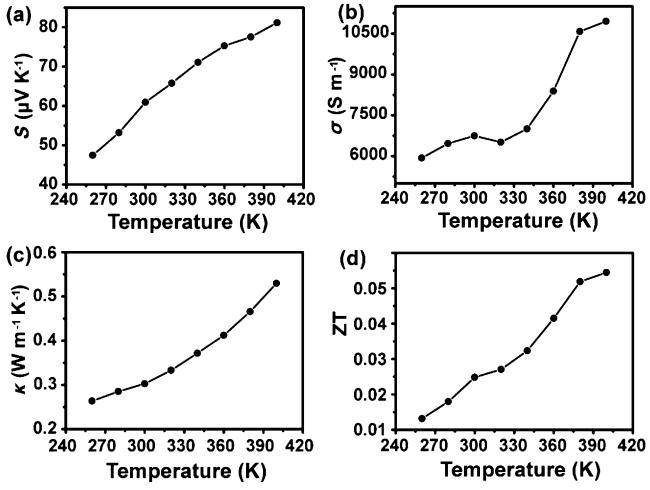

Figure 6. Temperature dependence of the a) Seebeck coefficient, b) electrical conductivity, c) thermal conductivity, and the d) figure of merit for wurtzite CZGSe NCs.

In addition to having favorable electrical transport properties, a good thermoelectric material must also have low thermal conductivity (κ). Figure 6c shows the temperature dependence of the thermal conductivity. Remarkably, the thermal conductivity of wurtzite CZGSe NCs was very low within the measured temperature range. According to the above-measured data, the ZT values of these materials were calculated based on the formula: $ZT = S^2\sigma T/\kappa$[34,35] and are plotted as a function of temperature in Figure 6d. Within the tested range, the ZT values increased continuously with temperature from 0.01 at 260 K to 0.05 at 400 K, which was larger than that of previously reported stannite CZGSe and equivalent to that of stannite $Cu_{2.15}Zn_{0.85}GeSe_{3.9}$ at similar temperatures.[18]

Conclusions

In summary, a facile hot-injection solution-phase synthesis method has been developed to synthesize high-quality CZGSe NCs with an unusual wurtzite structure. Furthermore, we performed a detailed thermodynamic and kinetic study of the phase transformation from the wurtzite structure into the stannite structure of CZGSe NCs during their colloidal synthesis, which revealed that wurtzite CZGSe, which represented the kinetic phase, could be prepared by using a kinetic growth process without phase transformation into the thermodynamic stable stannite structure. In addition, the thermoelectric properties of the as-prepared wurtzite CZGSe NCs were characterized, which demonstrated the potential use of wurtzite CZGSe as a thermoelectric material. The mechanistic results of this work allow for a rational manipulation of NCs with a desired crystal structure through adjusting the thermodynamics and kinetics, which can be easily achieved by simply tuning the reaction temperature or reaction time without using any additives and, more importantly, this effective and simple approach may be extended to effect control over structural transformations in the synthesis of other chalcogenide NCs.

Experimental Section

Synthesis of Wurtzite $Cu_2ZnGeSe_4$ Nanocrystals

In a typical synthesis, copper(II) acetate (0.2 mmol), zinc acetate (0.2 mmol), GeI_4 (0.1 mmol), and oleylamine (9 mL) were added into a 25 mL three-necked flask in air and degassed at about 120 °C for 30 min by bubbling with Ar gas under stirring. In a separate two-necked flask, diphenyl diselenide (0.2 mmol) and oleylamine (1 mL) were degassed at about 120 °C for 30 min by bubbling with Ar gas under stirring, then allowed to cool to 70 °C. The temperature of the former solution was heated to 230 °C and the solution of diphenyl diselenide and oleyla-

© 2013 Wiley-VCH Verlag GmbH & Co. KGaA, Weinheim

mine was quickly injected. The mixture soon turned brownish, thus indicating the formation of NCs, and was maintained for 1 h to allow the growth of NCs. Then, the flask was cooled to RT and excess EtOH was added to precipitate the NCs, which could be harvested through centrifugation at 9000 rpm for 3 min. The precipitates were washed three times with a mixture of EtOH and toluene. The final products were dispersed in toluene for further characterization.

Materials Characterization

TEM (Tecnai F20), high-resolution TEM (HRTEM, Tecnai F20), and SEM (JEOL 6701F, operating at 10 kV) were used to visualize the morphologies, sizes, and structures of the NCs. The phase and crystallographic structure of the NCs were characterized by powder X-ray diffraction (XRD) on a Regaku D/Max-2500 diffractometer with $Cu_{K\alpha 1}$ radiation ($\lambda = 1.54056$ Å). X-ray photoelectron spectroscopy data were recorded on an ESCALab220i-XL electron spectrometer (VG Scientific) by using 300 W $Al_{K\alpha}$ radiation.

Thermoelectric Measurements

The same synthetic procedure was scaled up for the production of a few grams of the nanoparticles. In the scaled-up synthetic procedure, 10-times larger amounts of the precursor and the solvent were used. The organic surfactants were removed by using the procedure mentioned below before the fabrication of bulk samples for the thermoelectric measurements. Briefly, as-prepared wurtzite $Cu_2ZnGeSe_4$ NCs were dispersed in MeOH and stirred vigorously for 48 h. Washed final NCs products were collected by centrifugation at 7000 rpm for 2 min; these NCs could not be redispersed in toluene, thus confirming a high degree of surfactant removal. The final products were dried under vacuum at 65 °C for 12 h. After the treatment, the NCs were pressed into compressed cuboid shapes for the thermopower-related tests. The Seebeck coefficients, electrical conductivities, and thermal conductivities were measured on a SB-100 Seebeck Measurement System (MMR Tech.), a KEITHLEY 2002 Multimeter (Keithley Instrument Inc.), and a TCi Thermal Conductivity Analyzer (C-THERM Tech.), respectively.

Acknowledgements

This work was supported by the National Natural Science Foundation of China (51225204, 21121063, and 91127044), the National Key Project on Basic Research (2011CB935700, 2012CB932900, and 2011CB932300), and the Chinese Academy of Sciences.

[1] A. Shavel, D. Cadavid, M. Ibáñez, A. Carrete, A. Cabot, *J. Am. Chem. Soc.* **2012**, *134*, 1438–1441.
[2] L. Shi, C. Pei, Y. Xu, Q. Li, *J. Am. Chem. Soc.* **2011**, *133*, 10328–10331.
[3] W.-C. Hsu, B. Bob, W. Yang, C.-H. Chung, Y. Yang, *Energy Environ. Sci.* **2012**, *5*, 8564–8571.
[4] W. Yang, H.-S. Duan, B. Bob, H. Zhou, B. Lei, C.-H. Chung, S.-H. Li, W. W. Hou, Y. Yang, *Adv. Mater.* **2012**, *24*, 6323–6329.
[5] W. Ki, H. W. Hillhouse, *Adv. Energy Mater.* **2011**, *1*, 732–735.
[6] H. Yang, L. A. Jauregui, G. Zhang, Y. P. Chen, Y. Wu, *Nano Lett.* **2012**, *12*, 540–545.
[7] F.-J. Fan, Y.-X. Wang, X.-J. Liu, L. Wu, S.-H. Yu, *Adv. Mater.* **2012**, *24*, 6158–6163.
[8] A. Fairbrother, E. García-Hemme, V. Izquierdo-Roca, X. Fontané, F. A. Pulgarín-Agudelo, O. Vigil-Galán, A. Pérez-Rodríguez, E. Saucedo, *J. Am. Chem. Soc.* **2012**, *134*, 8018–8021.
[9] S. C. Riha, B. A. Parkinson, A. L. Prieto, *J. Am. Chem. Soc.* **2009**, *131*, 12054–12055.
[10] S. C. Riha, B. A. Parkinson, A. L. Prieto, *J. Am. Chem. Soc.* **2011**, *133*, 15272–15275.
[11] K. Ramasamy, M. A. Malik, P. O'Brien, *Chem. Commun.* **2012**, *48*, 5703–5714.
[12] X. Lu, Z. Zhuang, Q. Peng, Y. Li, *Chem. Commun.* **2011**, *47*, 3141–3143.
[13] J.-J. Wang, J.-S. Hu, Y.-G. Guo, L.-J. Wan, *NPG Asia Mater.* **2012**, *4*, e2.
[14] Y. Wu, Y. Cui, L. Huynh, C. J. Barrelet, D. C. Bell, C. M. Lieber, *Nano Lett.* **2004**, *4*, 433–436.
[15] J.-J. Wang, D.-J. Xue, Y.-G. Guo, J.-S. Hu, L.-J. Wan, *J. Am. Chem. Soc.* **2011**, *133*, 18558–18561.
[16] G. Li, Y. Jiang, Y. Wang, C. Wang, Y. Sheng, J. Jie, J. A. Zapien, W. Zhang, S.-T. Lee, *J. Phys. Chem. C* **2009**, *113*, 17183–17188.
[17] M. Ibáñez, R. Zamani, W. Li, D. Cadavid, S. Gorsse, N. A. Katcho, A. Shavel, A. M. López, J. R. Morante, J. Arbiol, A. Cabot, *Chem. Mater.* **2012**, *24*, 4615–4622.
[18] M. Ibáñez, R. Zamani, A. LaLonde, D. Cadavid, W. Li, A. Shavel, J. Arbiol, J. R. Morante, S. Gorsse, G. J. Snyder, A. Cabot, *J. Am. Chem. Soc.* **2012**, *134*, 4060–4063.
[19] W. G. Zeier, A. LaLonde, Z. M. Gibbs, C. P. Heinrich, M. Panthöfer, G. J. Snyder, W. Tremel, *J. Am. Chem. Soc.* **2012**, *134*, 7147–7154.
[20] G. M. Ford, Q. Guo, R. Agrawal, H. W. Hillhouse, *Chem. Mater.* **2011**, *23*, 2626–2629.
[21] M. Zebarjadi, K. Esfarjani, M. S. Dresselhaus, Z. F. Ren, G. Chen, *Energy Environ. Sci.* **2012**, *5*, 5147–5162.
[22] C. Xiao, X. Qin, J. Zhang, R. An, J. Xu, K. Li, B. Cao, J. Yang, B. Ye, Y. Xie, *J. Am. Chem. Soc.* **2012**, *134*, 18460–18466.
[23] C. Xiao, J. Xu, K. Li, J. Feng, J. Yang, Y. Xie, *J. Am. Chem. Soc.* **2012**, *134*, 4287–4293.
[24] M. Ibáñez, D. Cadavid, R. Zamani, N. García-Castelló, V. Izquierdo-Roca, W. Li, A. Fairbrother, J. D. Prades, A. Shavel, J. Arbiol, A. Pérez-Rodríguez, J. R. Morante, A. Cabot, *Chem. Mater.* **2012**, *24*, 562–570.
[25] G. Hong, J. T. Robinson, Y. Zhang, S. Diao, A. L. Antaris, Q. Wang, H. Dai, *Angew. Chem.* **2012**, *124*, 9956–9959; *Angew. Chem. Int. Ed.* **2012**, *51*, 9818–9821.
[26] D.-J. Xue, J.-J. Wang, Y.-Q. Wang, S. Xin, Y.-G. Guo, L.-J. Wan, *Adv. Mater.* **2011**, *23*, 3704–3707.
[27] M. Ibáñez, R. Zamani, W. Li, A. Shavel, J. Arbiol, J. R. Morante, A. Cabot, *Cryst. Growth Des.* **2012**, *12*, 1085–1090.
[28] Y. Yin, S. Xin, L. Wan, C. Li, Y. Guo, *Sci. China Chem.* **2012**, *55*, 1314–1318.
[29] D.-J. Xue, J. Tan, J.-S. Hu, W. Hu, Y.-G. Guo, L.-J. Wan, *Adv. Mater.* **2012**, *24*, 4528–4533.
[30] A. L. Washington, M. E. Foley, S. Cheong, L. Quffa, C. J. Breshike, J. Watt, R. D. Tilley, G. F. Strouse, *J. Am. Chem. Soc.* **2012**, *134*, 17046–17052.
[31] L. Li, Z. Chen, Y. Hu, X. Wang, T. Zhang, W. Chen, Q. Wang, *J. Am. Chem. Soc.* **2013**, *135*, 1213–1216.
[32] W. Li, C. Zhao, B. Zou, X. Zhang, J. Yu, X. Zhang, J. Jie, *CrystEngComm* **2012**, *14*, 8124–8127.
[33] A. Cao, J. Hu, L. Wan, *Sci. China Chem.* **2012**, *55*, 2249–2256.
[34] Y. Sun, P. Sheng, C. Di, F. Jiao, W. Xu, D. Qiu, D. Zhu, *Adv. Mater.* **2012**, *24*, 932–937.
[35] Q. Zhang, Y. Sun, F. Jiao, J. Zhang, W. Xu, D. Zhu, *Synth. Met.* **2012**, *162*, 788–793.

Received: March 28, 2013
Published online: June 26, 2013

 © 2013 Wiley-VCH Verlag GmbH & Co. KGaA, Weinheim